10th International Conference on Fracture Mechanics of Concrete and Concrete Structures
FraMCoS-X
G. Pijaudier-Cabot, P. Grassl and C. La Borderie (Eds)
https://doi.org/10.21012/FC10.235353

STUDY OF THE EFFECT OF FLAX FIBERS ON THE FRACTURE BEHAVIOR OF EARTH CONCRETE BY SIMULTANEOUS APPLICATION OF DIGITAL IMAGE CORRELATION AND ACOUSTIC EMISSION

N. KOUTA[*], J. SALIBA[*], B. EL OIFI[*] AND N. SAIYOURI[*]

[*] Université de Bordeaux, UMR 5295,
Institut de Mécanique et d'Ingénierie (I2M),
Département de Génie Civil et Environnementale (GCE),
33405, France
E-mail : nathalie.kouta@u-bordeaux.fr

Key words: Earth concrete, Flax Fibers, Cracks, Digital Image Correlation, Acoustic Emission

Abstract: Nowadays, construction using natural materials such as earth-based concrete is of major interest for a sustainable society and in response to the challenges of global warming. These materials allow a significant reduction of CO2 and energy consumption in the production process. However, the presence of fine particles in earth concrete makes it sensitive to plastic shrinkage and consequently to cracking risk. Thus, flax fibers have been added to earth concrete to enhance its properties and to prevent the appearance of shrinkage cracking. The effect of adding flax fibers in different percentages (0%, 0.3% and 0.6%) and lengths (12 mm, 24 mm, 50 mm) on fracture properties of earth concrete has been studied. Compressive tests have been conducted on cubic specimens of 10x10x10 cm^3 at 7, 28 and 180 days. Flexural tests have been also realized on prismatic specimens at 28 days. Those tests have been monitored simultaneously with the digital image correlation (DIC) and the acoustic emission (AE) techniques. The results show that the compressive strength, the tensile strength and the AE activity increased with the addition of fibers. Crack displacement fields of hardened concrete and the AE events showed also the development of multi-cracking with the addition of fibers. Those later enhanced the ductility of earth concrete due to fibers bridging of the cracks.

1 INTRODUCTION

During the last decade, a large quantity of natural resources has been consumed by the construction sector and a large quantity of waste and an intensive emission of CO2 have been generated [1]. These productions have a significant impact on the environment and participate in climate change [2]. For this reason, the need of using ecological and sustainable materials is becoming an obligation in the construction fields. The ecological earth concrete can be an alternative to conventional concrete for structures that do not require high mechanical performances but rather thermal and acoustic characteristics [3].

Earth constructions have been used since millions of years in different forms. They are essentially composed of a raw material, the soil which is a non-manufactured, recyclable, local and inexpensive material [4]. The stabilization of soil concrete has been first realized with lime then with cement and other binders (fly ash, silica fume, geopolymer, etc.) [5-6]. During the last recent years, researches have focused on finding easier and more common methods to use these materials in the construction fields due to their properties and ecological aspects [5].

Earth materials present a high shrinkage rate and thus a cracking sensibility during drying when concrete is restrained [7]. The addition of natural or vegetable fibers may decrease the shrinkage rate. In addition, the good combination between these fibers and clay matrix prevents the propagation of cracks and contributes in improving the strength and the ductility of earth concrete [8]. Natural fibers are widely used in earth construction. These fibers vary in type, chemical properties, shape, size, source, strength, elasticity, water absorption rate and their cohesion degree to the earth concrete. Several studies have tested the effect of different types of fibers on the physical and mechanical properties of earth-based concrete [9], [10]. The effect of these fibers on the compressive and tensile strength is not comparable between the different studies due to the variability of the specific percentages of fibers and to the different materials used in each study. These mechanical characteristics are affected by the properties of the natural fibers used especially their ratios in the formulation and their lengths.

In this study the choice of using Flax fibers was based on several criteria. Flax fibers are natural ecological fibers with a high tensile strength and they have good thermal and acoustic properties.

The aim of this paper is to study the effect of flax fiber percentages and lengths on the fracture behavior during compressive and flexural tests using the digital image correlation and the AE technique in order to have a better understanding of the different damage mechanisms.

2 EXPERIMANTAL PROGRAM

2.1 Materials

The soil used in this study is an artificial soil in order to limit the variability of natural soil. The artificial soil is composed of 30% of bentonite clay (75% of smectites, 15% of elites and 10% of Kaolinite) and 70% of sand to have a good compactness. The characteristics of the bentonite supplied from Lafaure are presented in (Table 1). This mixture is treated by two types of hydraulic binder lime and cement. The lime used is the hydraulic lime (NHL5) in accordance with the European standard EN 459-1 with a percentage of 3% of the clay-sand mixture. This percentage is fixed based on other studies in the literature that showed that 2% to 4% of lime are sufficient to stabilize the soil [11]. The cement used is CEM 1, 52.5 N PM-CP2 according to NF EN197-1 standard (Table 2). The percentage of cement is equal to 8% of the formulation mass in order to ensure a minimal strength [12].

Table 1: Bentonite clay properties

Naturel water content	Liquid limit	Plastic limit
6,7%	84,6%	29,2%

Table 2: Mineralogical composition of cement

Main components	Percentage (%)
C3S	65
C2S	12
C4AF	6
C3A	12

Figure 1 presents the grain size distribution of sand and bentonite. This analysis has been carried out by sieving according to the standard (NFP P 94-041) for particles having a diameter greater than 0.08 mm and by sedimentation according to the standard (NF P94-057) for fine particles (<0.08 mm). Bentonite and sand are mixed together at the beginning to ensure a certain homogeneity. Then, the lime and the cement has been added to the dry mixture before the addition of water and superplasticizer (Tempo 10).

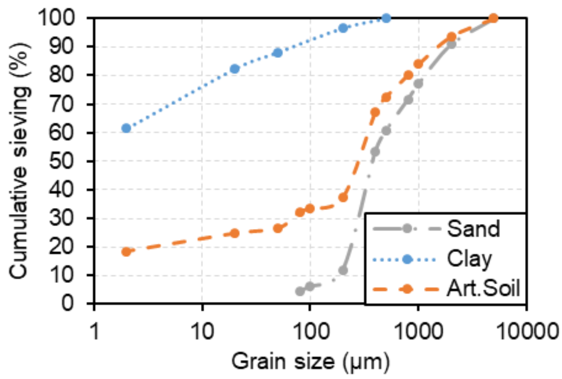

Figure 1: Grain size distribution of Sand, Clay and the resultant artificial soil

2.2 Sample formulations

Seven formulations have been tested by varying the percentage of fibers (0; 0.3 and 0.6%) and their lengths (12; 24 and 50 mm). Table 3 presents the components of these formulations. The quantity of fibers added is subtracted from the artificial soil mass to keep an equivalent solid mass. The effective water to Binder ratio has been kept constant and equal to 0.45. Additional water has been added to take into account the water absorbed by flax fibers.

Slump test has been also conducted at early age on fresh concrete according to EN 12350-2. The results show (Figure 2) that even if the water absorbed by fibers is taken into consideration, the effect of adding fibers on the workability of the concrete remains important. The increase of the percentage of fibers decreases the slump of this concrete.

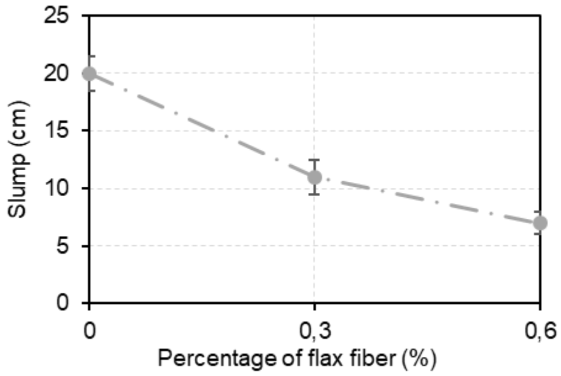

Figure 2: Slump test results

2.3 Methods

2.3.1. Compressive and flexure strength test

Unconfined compressive and flexural tests have been conducted using an electromechanical machine with a capacity of 100 kN. Tests have been plotted with a constant loading displacement rate of 0.6 mm/min and 0.15 mm/min respectively.

For the compressive strength, the test has been realized on cubic 10×10×10 cm^3 specimens at the age of 7, 28 and 180 days and for the flexural tests on a 7×7×28 cm^3 specimens at the 28th day and the 180th day. These specimens have been cured in a climatic chamber with a relative humidity of 80-95%.

Figure 3: Compressive and flexural tests setup

2.3.2. Digital image correlation technique

The compressive and flexural tests have been monitored with the digital image correlation technique in order to have more information on the effect of fibers on the fracture process.

A speckle pattern of black and white paint has been sprayed onto the surface of the captured specimen to improve the displacement resolution. Specimen images have been captured using a digital camera with a resolution of 2452 × 2056 pixels. Mention that two lamps have been used to improve the luminosity of the images. Images have been taken at a rate of one image per second during the tests. The treatment of the images has been realized using the commercial Vic 2D software with a resolution of 0.047 mm per pixel for the compressive test and 0.1 mm per pixel for the flexural test.

Table 3: Formulations.

Components (kg/m3)	Sand	Bentonite	Cement	Lime	Effective water	Super-plasticizer	Flax fibers
SA0F0	931	405	152	34.2	83.8	1.6	0
SA03F12/24/50	929	401	152	34.2	83.8	1.6	5.7
SA06F12/24/50	925	399	152	34.2	83.8	1.6	11.4

2.3.3. Acoustic emission technique

The tests have been also monitored with the AE technique. The AE system consists on eight channel AEWIN system with a general-purpose interface bus and a system for data storage analysis. A 3D localisation algorithm has been used for the localization of AE events. The importance of this technique is to investigate the local damage in the materials [13]. In this study, 8 piezoelectric sensors of type R15a were used (Figure 4). These sensors have a frequency range between 50 – 200 kHz with a resonance frequency of 150 kHz. Transducers were placed on two opposite sides of the specimen using silicon grease that served as a coupling agent. For the compressive test, they covered all the surfaces. However for the flexure test, the transducers were placed around the expected location of the fracture zone. The detected signals were amplified with a 40 dB gain differential amplifier. The acquisition system was calibrated before each test using a pencil lead break procedure. Signal descriptors such as rise time, counts, energy, duration, amplitude, average frequency and counts to peak were captured and calculated by AEwin system.

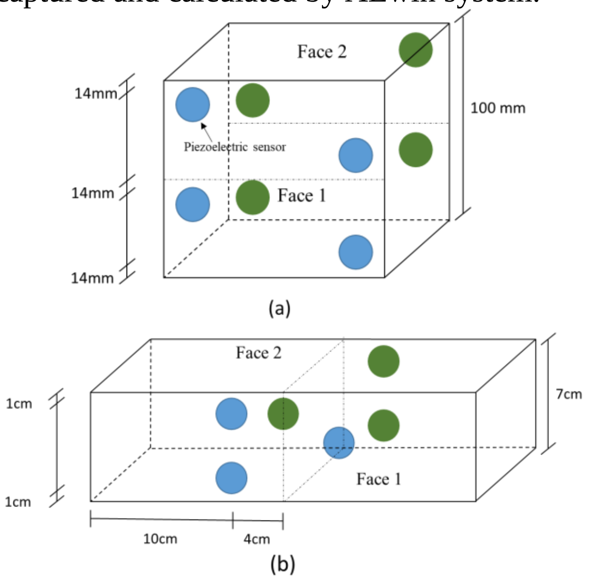

Figure 4: AE transducers position for the (a) compressive and (b) flexural specimens (blue sensors-face 1, green sensors-face 2).

3 RESULTS AND DISCUSSIONS

3.1 Compressive tests

Three specimens have been tested for each mixture to study the repeatability of the different formulations. Figure 5 shows the stress-strain curves obtained for the formulations containing 0; 0.3 and 0.6% of flax fiber of 12 mm length. A more ductile behavior was observed for fiber formulations with a higher deformation capacity and fracture energy at the rupture phase. This could be due to the high compressibility of plant fibers which generate a very high residual resistance.

Figure 6 presents the maximum compressive strength at 7, 28 and 180 days. At the 7th and the 28th days, the maximum compressive strength is higher with the addition of fibers and is more significant with the addition of 0.6% of flax fibers that prevent the spreading of cracks [6].

The compressive strength increases significantly even after 28 days. It doubled at 180 days for the formulations with 0.6% of fibers and was equal to 2.4 times for the formulations without fibers. This increase may be due to pozzolanic and hydration reactions related to lime and cement. These reactions increase the cohesive force between the clay particles and thus the mechanical properties of earth concrete [14], [15].

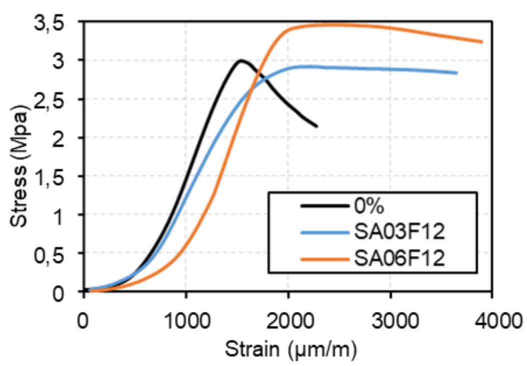

Figure 5: Stress-Strain curves for 0; 0.3 and 0.6% of flax fibers at the age of 28 days.

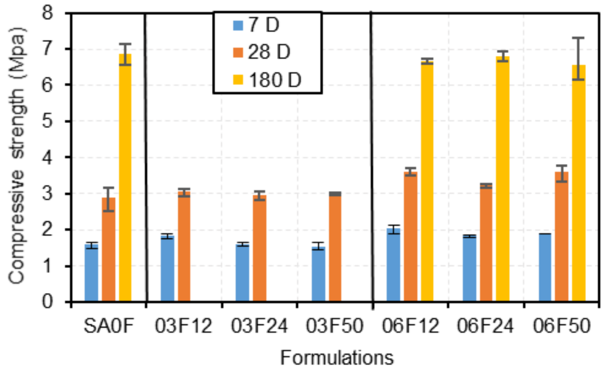

Figure 6: Compressive strengths of the seven specimen formulations at 7, 28 and 180 days.

The elastic modulus has been also calculated for each formulation (Table 4). The results show that the elastic modulus decreases with the addition of fibers to earth concrete. For the formulations with fibers, the elastic modulus increases while increasing the length of the flax fibers. In addition, the increase of the percentage of flax fibers in the formulation from 0.3 to 0.6% decreases the elastic modulus due to the soft and flexible properties of flax fibers.

Figure 7 shows the evolution of the strain field and the failure behavior for specimens with 0; 0.3 and 0.6 % of flax fibers with a length of 12 mm at 30%, 60%, 80%, 90%, 100% before the peak and at 90% in the softening part. A uniform strain field has been initially observed; then, the deformations begin to localize due to different stress concentration mechanisms. A brittle behavior has been observed for the formulations without fibers, accompanied with the propagation of a large crack from the bottom to the top of the specimen during the compressive test. However, for specimens containing fibers, a multi cracking has been observed and the lengths of cracks are way smaller than those obtained with the formulation without fibers. In addition, and as presented in the stress-strain curves, specimens containing fibers have shown a more important compressibility and ductility with a more important post peak region due stress redistribution and load transfer between the fibers and the matrix and to the bridging effect of fibers. Thus, the addition of flax fibers improved greatly the ductility, the compressibility and the fracture energy of earth concrete.

Compressive tests have been also monitored with AE technique. Figure 8 shows the correlation between the stress level and the cumulative number of AE hits. Four phases of evolution can be distinguished. In the first phase (stress < 0.3 Mpa), a high rate has been observed which may be due to stress concentration at the support level. At the second phase, the number of hits increases slowly indicating the initiation of micro cracks and progressively of the damage. The cumulative number of AE signals increases rapidly after the peak, indicating the propagation of multi-cracking as shown by the DIC technique. This rate decreases later (phase 4) indicating the stable propagation of the crack. Note here that the cumulative number of AE hits increases with the percentage of fibers. Figure 9 shows the strain field obtained with DIC in correlation with AE localization map for SA03F12. AE events are distributed along the entire surface indicating a diffuse damage as shown with DIC.

Table 4: Elastic Modulus.

Formulations	SA0F	SA03F12	SA03F24	SA03F50	SA06F12	SA06F24	SA06F50
Elastic modulus (Mpa)	3100	1520	1820	2670	1460	1630	2480

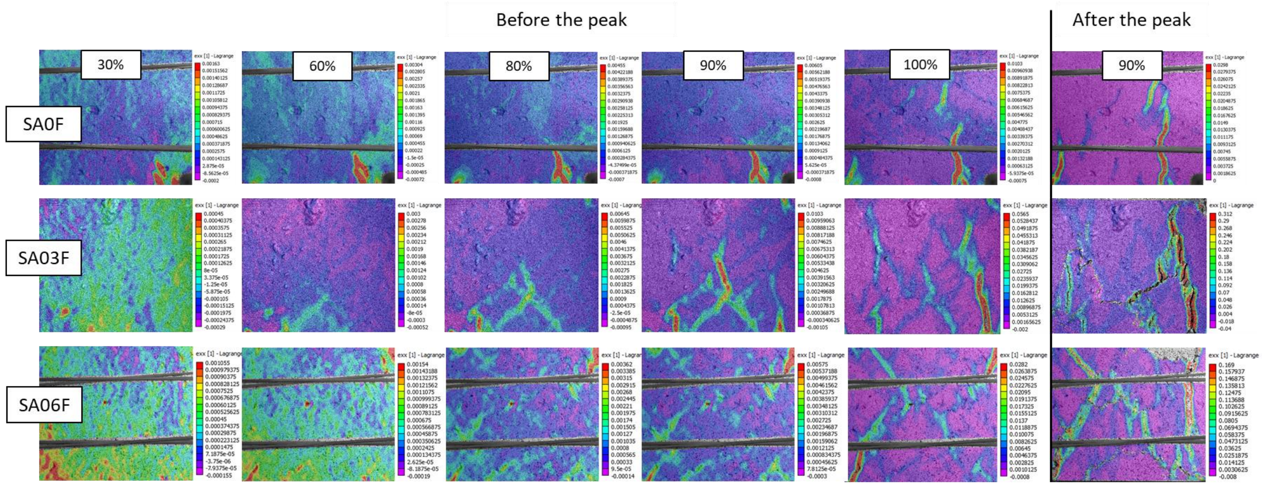

Figure 7: Evolution of the strain field of specimens with 0; 0.3 and 0.6 % of flax fibers with a length of 12 mm for different loading levels at 28 days.

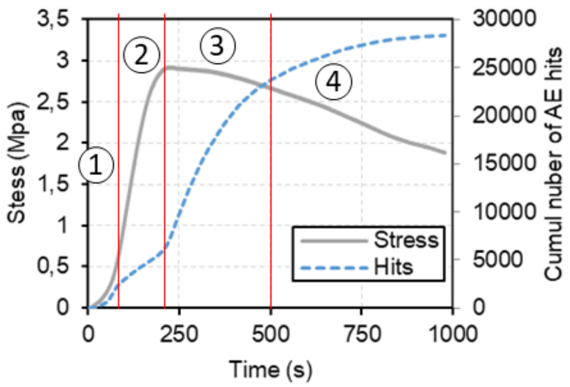

Figure 8: Correlation between the stress and the cumulative number of AE hits formulated with 0.3% of fibers at 28 days.

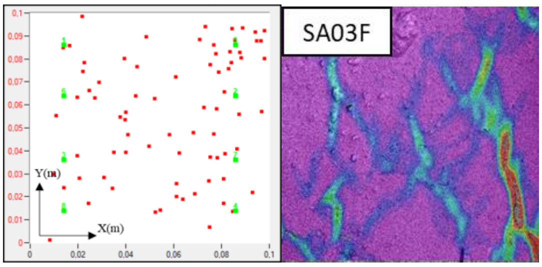

Figure 9: Comparison between the localization map of AE events and the strain distribution using DIC for SA03F12 at 28 days.

3.2 Flexural tests

Flexural tests have been also conducted on prismatic specimens for all the formulations to evaluate the effect of the flax fibers on the flexural strength and the ductility of earth concrete. Three specimens have been tested for each mixture. These tests have been realized at the age of 28 and 180 days of curing. Figure 10 presents the peak flexural strength for the seven studied formulations. A significant difference between the three specimens tested at the age of 28 and 180 days has been observed for the formulation with long fibers (24 and 50 mm). This may be due to the variability in the distribution of fibers in the mixture and to the flexibility of long flax fibers that can take different shapes and positions inside the specimen. The flexural strength increases slightly with the addition of fibers at the age of 28 and 180 days. However, the difference between the flexural strength at 28 and 180 days was less important than that obtained with compressive strength where it was multiplied by 1.4 approximatively.

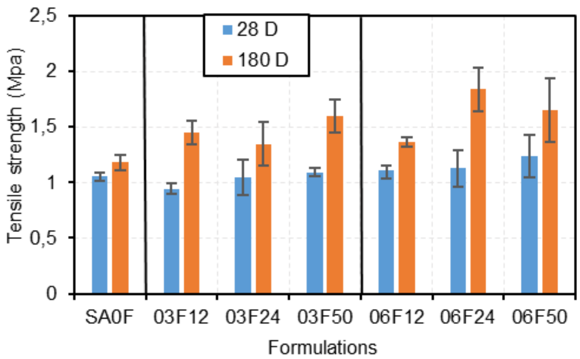

Figure 10: Effect of the percentage and the length of flax fibers on the flexural strength of earth concrete at the age of 28 and 180 days.

Figure 11 presents the load in function of the mid span deflection for the formulations with different percentages of flax fibers (0, 0.3, 0.6%). Specimens without fibers presented a brittle failure followed by a propagation of one crack from the bottom to the top of the specimen and a high strength loss after reaching the peak. For the mixtures containing fibers, the presence of flax fibers helped to bridge the formed cracks and to avoid any brittle rupture by redistributing the loads, which led to a ductile failure. This can be also seen by the increase of the surface below the load-deflection curve after the peak indicating the increase of the specific fracture energy. This energy was equal to 52 N/m for non-fibered earth concrete due to the brittle drop of the force and increased to 220 N/m and 258 N/m for specimens containing 0.3% and 0.6% of fibers respectively.

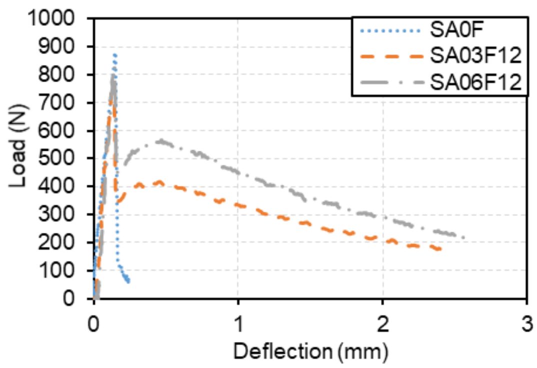

Figure 11: Load- mid span deflection curves for specimens with 0; 0.3 and 0.6% of flax fibers at 28 days.

The AE technique has also allowed to capture the crack localization during the flexure test. The energy emitted during the crack formation is transmitted in the form of an elastic wave to the sensors presented on the external surface of the earth concrete specimen. AE events localization was realized based on the arrival times of the first wave at each sensor and their respective velocity in concrete specimen. Once the arrival time is detected, a least-square method is used to estimate the AE event location [17]. Figure 12 presents the localization maps of AE events at the end of the test for earth concrete without fibers and with 0.6% of fibers with a length of 12 mm at the age of 28 days. A small number of AE events have been generated for specimens without fibers compared to the ones containing 0.6% of fibers which may be due to different mechanisms in the post peak region that adsorb additional energy. In fact, fibers can change the orientation or the crack path in the matrix and induced many mechanisms such as micro-cracking, crack bridging and stress distribution. Note that the AE energy is more important for earth concrete with fibers in correlation with the fracture energy.

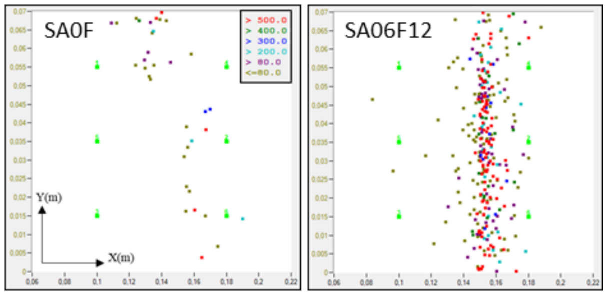

Figure 12: Localization map for specimens with 0; and 0.6% of flax fibers at 28 days.

Figure 13 presents the localization maps of AE events in correlation with the strain fields for different loading levels for SA06F12 at the age of 180 days. During the elastic phase, no AE events have been generated. After the initiation of the crack, the number of AE events increased due to the effect of fibers bridging and the increase of the micro cracks at the interface between fibers and matrix. This crack does not directly result in the complete rupture of the specimen. The width of the crack increased with time with the incensement of the deflection of the specimen. Thus, adding fibers has led to a slow crack propagation in the material which is not the case for the formulation without fibers.

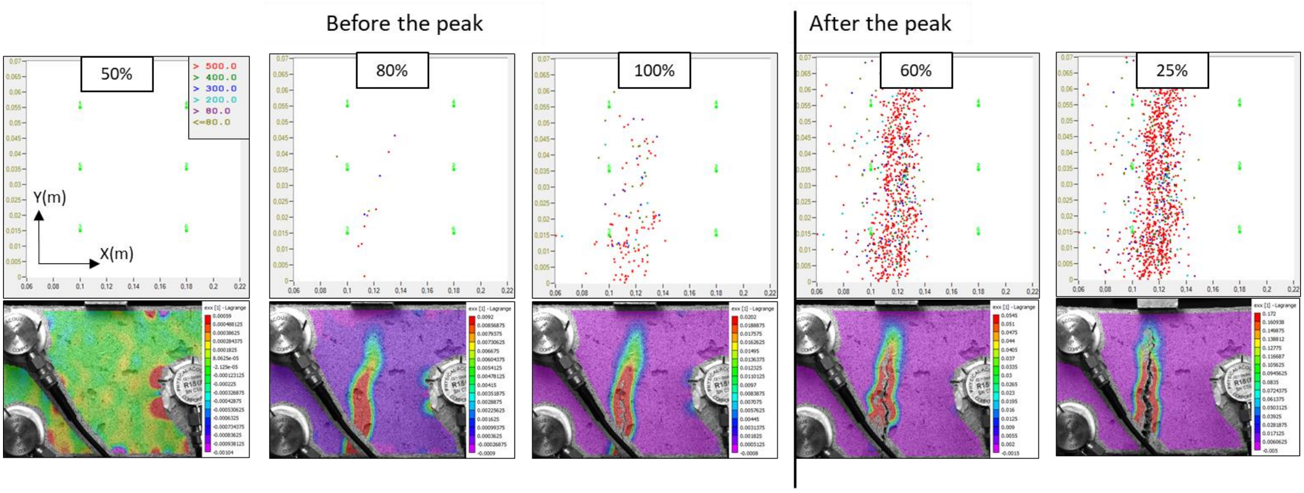

Figure 13: Evolution of the localization maps of AE events in correlation with the strain fields for the formulation SA06F12 at 180 days.

Figure 14 presents the correlation between the load level and the cumulative number of acoustic emission hits for the formulations with 0.6% and without fibers. This figure shows that the rate of the AE activity is slow before the peak. In fact, few AE hits are generated at the beginning in the elastic phase for the formulation without fibers and then increased slowly due to stress concentration and micro cracking. For specimens without fibers, a brittle rupture has been observed at the peak accompanied with the emission of a high number of AE hits. For the formulations with fibers, the number of AE hits increased progressively after the peak indicating the formation of micro cracks around the principal crack due to crack bridging and a higher fracture process zone. It's clear that the number of AE events and hits is much more important for the formulations containing fibers in comparison with the one without fibers (400 hits for SA0F and more than 5000 hits for SA06F12). This increase in the number of AE hits can be attributed to different damage mechanisms as micro-cracking at the interface between the fibers and the cement matrix, bridging, friction...

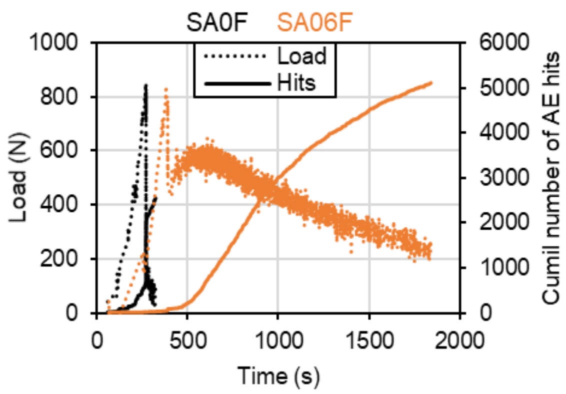

Figure 14: Correlation between the load and the cumulative number of AE hits for SA0F and SA06F12 at 28 days.

4 Conclusions

This paper presents the effect of the incorporation of different percentages and lengths of flax fibers on the fracture behavior of earth concrete using the digital image correlation and the acoustic emission techniques. The results show that the addition of fibers in the mixture increased slightly the compressive strength. The compressive strength doubled for the tested specimens at the age of 180 days for all the formulations. In addition, the incorporation of fibers increased the ductility of earth concrete during the compressive and flexural tests which was manifested by a multi crack propagation. A higher compressibility has been also observed by adding fibers to the mixture. The AE activity increased with the addition of fibers indicating additional damage mechanisms as micro-cracking and crack bridging that prevent the brittle failure of specimens.

Additional studies will be realized in the future in order to study the effect of fibers on the plastic shrinkage and the durability of the earth concrete.

5 References

[1] Dahlbo, H. et al., 2015. Construction and demolition waste management - A holistic evaluation of environmental performance. *J. Clean. Prod.* **107**: 333–341.

[2] Llatas, C., 2011. A model for quantifying construction waste in projects according to the European waste list. *Waste Manag.* **31**:1261–1276.

[3] Van Damme, H. and Houben, H., 2016. Earth concrete. Stabilization revisited. *Cem. Concr. Res.* **114**:90–102.

[4] Pacheco-Torgal, F. and Jalali, S., 2012. Earth construction: Lessons from the past for future eco-efficient construction. *Constr. Build. Mater.* **29**:512–519.

[5] Taallah, B. and Guettala, A., 2016. The mechanical and physical properties of compressed earth block stabilized with lime and filled with untreated and alkali-treated date palm. *Constr. Build. Mater.* **104**:52–62.

[6] Laborel-Préneron, A., Aubert, J. E., Magniont, C., Tribout, C. and Bertron, A., 2016. Plant aggregates and fibers in earth construction materials: A review. *Constr. Build. Mater.* **111**:719–734.

[7] Kanema, J.M., Eid, J. and Taibi, S., Tribout, C., 2016. Shrinkage of earth concrete amended with recycled aggregates and superplasticizer: Impact on mechanical properties and cracks. *Mater. Des.* **109**:378–389.

[8] Millogo, Y., Morel, J. C., Aubert, J. E. and Ghavami, K., 2014. Experimental analysis of Pressed Adobe Blocks reinforced with Hibiscus cannabinus fibers. *Constr. Build. Mater.* **52**:71–78.

[9] Bouhicha, M., Aouissi, F. and Kenai, S., 2005. Performance of composite soil reinforced with barley straw. *Cem. Concr. Compos.* **27**:617–621.

[10] Mohamed, A. E. M. K., 2013. Improvement of swelling clay properties using hay fibers. *Constr. Build. Mater.* **38**:242–247.

[11] Khattab, S.A. et al. and Al-Mukhtar, M., 2007. Long-term stability characteristics of a lime-treated plastic soil. *Mater. Civ. Eng.* **19**:358–366.

[12] Anagnostopoulos, C.A., 2015. Strength properties of an epoxy resin and cement-stabilized silty clay soil. *Appl. Clay Sci.* **114**:517–529.

[13] Prem, P.R. and Murthy, A. R., 2017. Acoustic emission monitoring of reinforced concrete beams subjected to four-point-bending. *Appl. Acoust.* **117**:28–38.

[14] Bell, F.G., 1996. Lime stabilization of clay minerals and soils. *Eng. Geol.* **42**:223–237.

[15] Locat, M.C.J. and Bérubé, M. C. J., 1990. Laboratory investigation on the lime stabilization of sensitive clays: shear strength development. *Can. Geotech. J.* **27**:294–304.

[16] Yetgin, Ş., Çavdar, Ö. and Çavdar. A., 2008. The effects of the fiber contents on the mechanic properties of the adobes. *Constr. Build. Mater.* **22**:222–227.

[17] Kurz, J. H., 2015. New approaches for automatic threedimensional source

localization of acoustic emissions – Applications to concrete specimens. *Ultrasonics*. **63**:155–162.